PROCESSING OF BIOCERAMIC IMPLANTS VIA FUSED DEPOSITION PROCESS

Susmita Bose, Marisol Avila and Amit Bandyopadhyay

School of Mechanical and Materials Engineering
Washington State University
Pullman, WA 99164-2920

Abstract

Porous ceramic structures have long been a subject of investigation as bone substitute. Most of these porous structures are typically made by techniques that result randomly arranged pores with a wide variety of pore sizes. In recent years, SFF methods are being used for the fabrication of porous bioceramic implants. Porous ceramic structures have been fabricated using indirect route where a polymeric mold is first created via fused deposition process. The mold was then infiltrated with ceramic slurry, dried and then subjected to a binder burn out and sintering cycle. In this paper, processing of 3D honeycomb porous alumina ceramic structures and some initial mechanical properties for bone implants will be discussed.

Introduction

Development of specially designed ceramics and composites for the repair and reconstruction of diseased or damaged parts of the human body have been revolutionized the quality of human life during last five decades [1-5]. A number of different materials have been utilized for these purposes in various forms including collagen, metals, metal alloys, ceramics, glasses, carbon based materials and composites of the above materials. Among them, ceramic based materials are considered the most suitable artificial graft material [6]. The ceramic materials that are used for these purposes are called *bioceramics*. These bioceramic materials may be inert in nature (such as alumina, zirconia, titania), bioactive (such as hydroxyapatite, bioactive glasses or bioactive glass-ceramics) or resorbable (such as tricalcium phosphate, calcium phosphate salts). Bioceramic implants can again be classified into two categories including dense bioceramics and microporous bioceramics [1]. The potential for ceramics as biomaterials relies upon their compatibility with the physiological environment. Bioceramics are compatible because they are composed of ions commonly found in physiological environment and of ions showing limited toxicity to body tissues. Moreover, these materials are resistant to microbial attack, pH changes and solvent conditions and stable with temperature changes [7]. Applications of bioceramic materials include restoration of material in dentistry, spinal fusion, bone filling, maxillofacial reconstruction and hip, knee or other bone replacements.

Among the various bone substitutes that are currently being used that include: (1) autograft (bone from the another location from the body of the same person), (2) allograft (human bone from dead body), (3) genograft (animal bone) and (4) bioceramic implant (artificial bone). Though autograft is probably the most suitable one, but it requires at least two operations and often causes problems with patient body from where the bone is taken (commonly hip or rib). In both, allograft and genograft, rejection by the patient body and diseases transmitted by the foreign bone are of serious concern for their applicability. Naturally, applications of artificial

implants are becoming more and more popular. The increasing demand for bioceramic implants is evident form the growth of this field. In 1997, total estimated business was over $50M and the projected sales for these implants for the year 2004 is over $150M.

In recent years, rapid prototyping (RP) or solid freeform fabrication (SFF) techniques have shown potential for the fabrication of controlled porosity bioceramic implants. Selective laser sintering (SLS) [8-9], 3-D printing [10-11], stereolithography [12], ceramic filled stereolithography [13] and fused deposition (FDM). [14] processes have already been utilized to demonstrate the feasibility of processing controlled porosity ceramic implants for biomedical applications. In this work, polymeric molds were fabricated using an FDM 1650. Molds were infiltrated with alumina ceramic slurry, dried and then subjected to a binder burn out and sintering cycle. Processing and initial mechanical characterization of 3D honeycomb porous alumina ceramic preforms are described in this paper.

Processing

Processing of porous 3D honeycomb alumina ceramic preforms consists of three different types of development and optimization work. They are: (1) mold design, (2) development of ceramic slurry composition and (3) binder burn out and sintering cycle development for green ceramic structures.

Mold Design

Molds were designed and fabricated by FDM 1650 using ICW-06 filament material. Initially, 1" tall and 1" diameter cylindrical molds were designed and fabricated with a (45/-45) raster filling and varying the raster gap from 0.010 to 0.030". Top 0.3" of the mold had only perimeter but no raster filling, which is also called lip, to hold excess ceramic slurry during infiltration. Bottom four layers of the mold had no raster gap to avoid leaking of slurry during infiltration. Road width was varied from 0.015 to 0.025". Combination of raster gaps and road width control the volume fraction of ceramics and its pore sizes in the preform. Figure 1a and b show the schematic of mold design and top view of a polymeric mold.

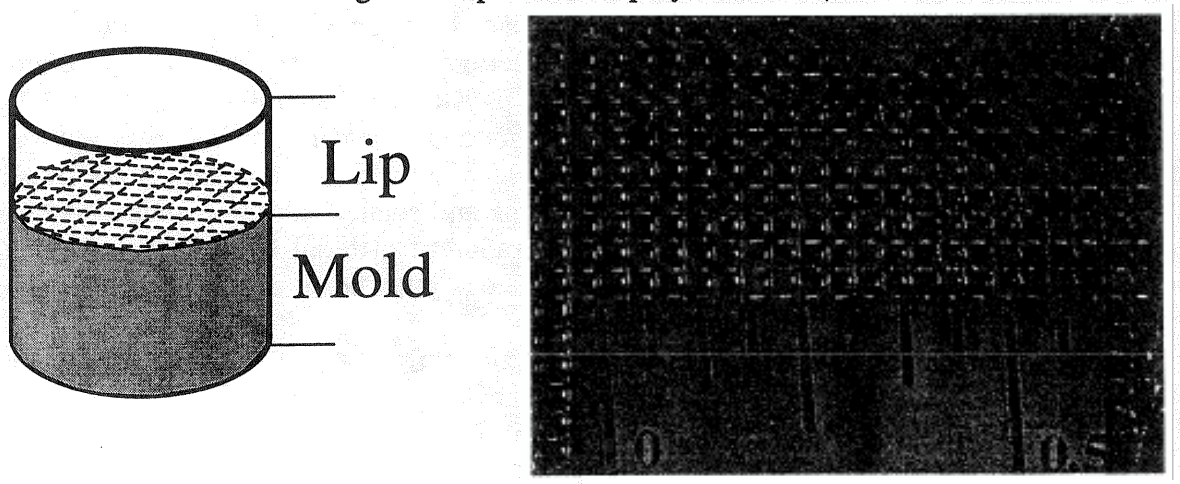

(a) (b)

Figure 1: (a) Schematic presentation of polymeric mold design. (b) Optical image of the top view of a polymeric mold made by FDM 1650 using ICW06 material (scale 0 - 0.5").

Development of Ceramic Slurry Composition

Development of ceramic slurry work started with different commercially available alumina powders. Finally most of the work has been performed with 10D and 30D alumina powders doped with 500 ppm of MgO from Baikowski International Corporation, N.C. Both 10D and 30D powders have submicron size particles (Sedigraph d_{50} for 10D = 0.45 μm and for 30D = 0.41 μm), but specific surface area for 30D powder is 26.6 m^2/gm compared to 8.6 m^2/gm for 10D. High surface area of the 30D powder is also evident from higher slurry

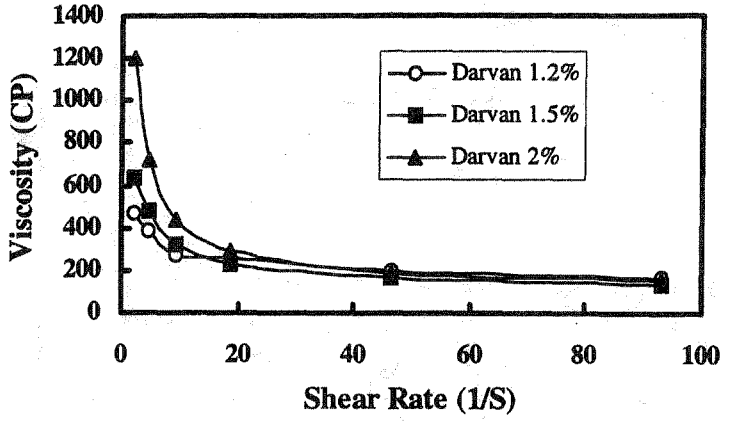

(a)

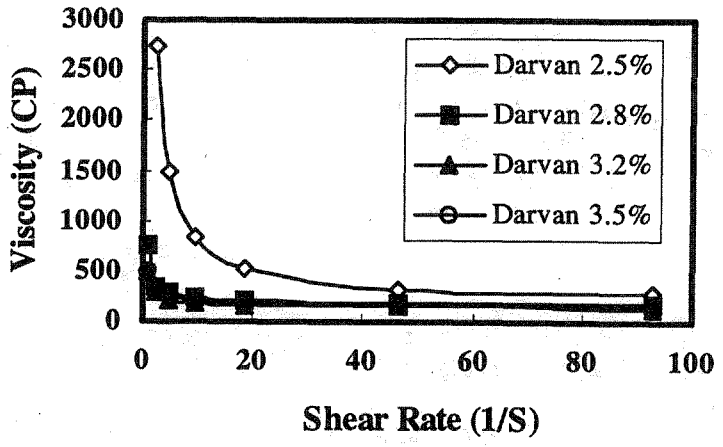

(b)

Figure 2: Effect of dispersant amount on the viscosity of ceramic slurry with (a) 10D and (b) 30D powders.

viscosity compared to 10D powder at similar solids loading. Brookfield Viscometer was used to determine the optimum wt% of dispersant needed for the preparation of water based ceramic slurry by measuring the viscosity at different shear rates for each solution. 1-Butanol (Fisher Scientific) was used as an antifoaming agent for this ceramic slurry. Darvan 821 (R.T. Vanderbilt & Co., Norwalk, CT) was used as a dispersant. For the 10D alumina powder, 1.5

wt% darvan was found to be optimum and beyond that it increased the viscosity of the slurry a little bit. Whereas for the 30D alumina powder the optimum dispersant amount was 3 wt%. The viscosity vs. shear rate plots at different dispersant wt% for both the powders are shown in Figures 2a and b.

Viscosity of 10D and 30D ceramic slurry compositions at a fixed shear rate of 46 (1/S) were measured with increasing solid loading. The wt% of antifoaming agent and dispersant in the slurry were kept constant. Figure 3 shows the plot of viscosity vs. solids loading for both the powders. For the 10D powder, up to 63 wt% solid loading could be achieved, but for the 30D powder it was only 55 wt%.

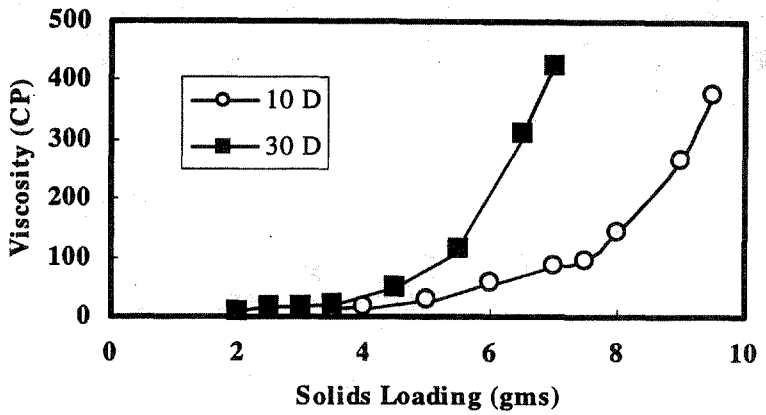

Figure 3: Effect of solids loading on the viscosity for 10D and 30D alumina ceramic powders.

For the present study, 10D and 30D both the powders were used to make water based ceramic slurry. Powder, antifoaming agent and dispersant were added to water and then mechanically stirred in a polyethylene boat for 10 minutes. The required amount of binder B-1035 (Rohm and Hass) was added to the mixture just before infiltration. Polymeric molds, produced via FDM, were infiltrated with the ceramic slurry using a vacuum oven. The infiltrated molds were dried at room temperature for 12 hours and then subjected to binder removal and sintering cycles.

Binder Removal and Sintering Cycle Development

Binder removal and sintering of dry ceramic powder loaded molds were carried out in a muffle furnace in furnace air environment. Samples were placed on top of a porous zirconia ceramic plate. Figure 4 shows the heating cycle. During the first part of the cycle (by 550^0C), polymeric mold material and the binder evaporates. A slower heating rate is necessary up to this point to avoid cracking or distortion of the part. At higher temperature, densification of alumina ceramic occurs. A final sintering temperature of 1600^0C and a hold time of 3 hours was used for all the samples.

Physical and Mechanical Characterization

The aim of this work was to investigate one of the most fundamental and general questions regarding bioceramic implants: what are the effects of pore size, pore volume and pore

distribution on the biomechanical properties of porous ceramic implants. During this initial part of the work, porous 3D honeycomb ceramic preforms were fabricated with various pore sizes and pore volumes. The 3D honeycomb structure has unique pore geometry that are inter-

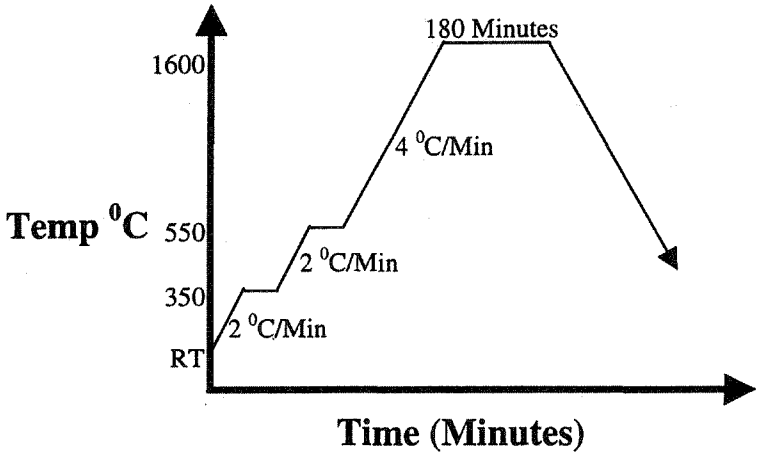

Figure 4: Schematic representation of the binder removal and sintering cycle for green ceramic parts.

connected in all three X, Y and Z directions. In this work, two types of ceramic preforms were fabricated. In the first type, the pore size was same in all the three directions or uniform pore geometry sample. But in the second type, pore sizes were different in X and Y compared to Z direction or non-uniform pore geometry. Similarly, a volume fraction gradient in porosity could also be achieved in pore distribution from top to bottom of the preform or from side to the center of the preform.

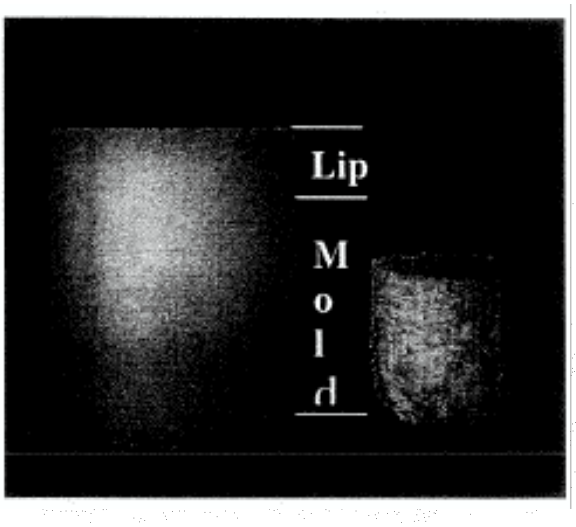

Figure 5: Optical photograph of a polymeric mold (with mold and lip) prepared via FDM and a sintered alumina ceramic preform.

Shrinkage is one of the most important factors during processing of these porous alumina ceramics. Initial data showed that linear shrinkage for the green to the sintered stage lie between

22 to 25%. Shrinkage data depends on the solids loading of the slurry and the particle size distribution of the ceramic powders. Figure 5 shows an optical photograph of a polymeric mold including the lip and a sintered ceramic preform fabricated using a similar mold.

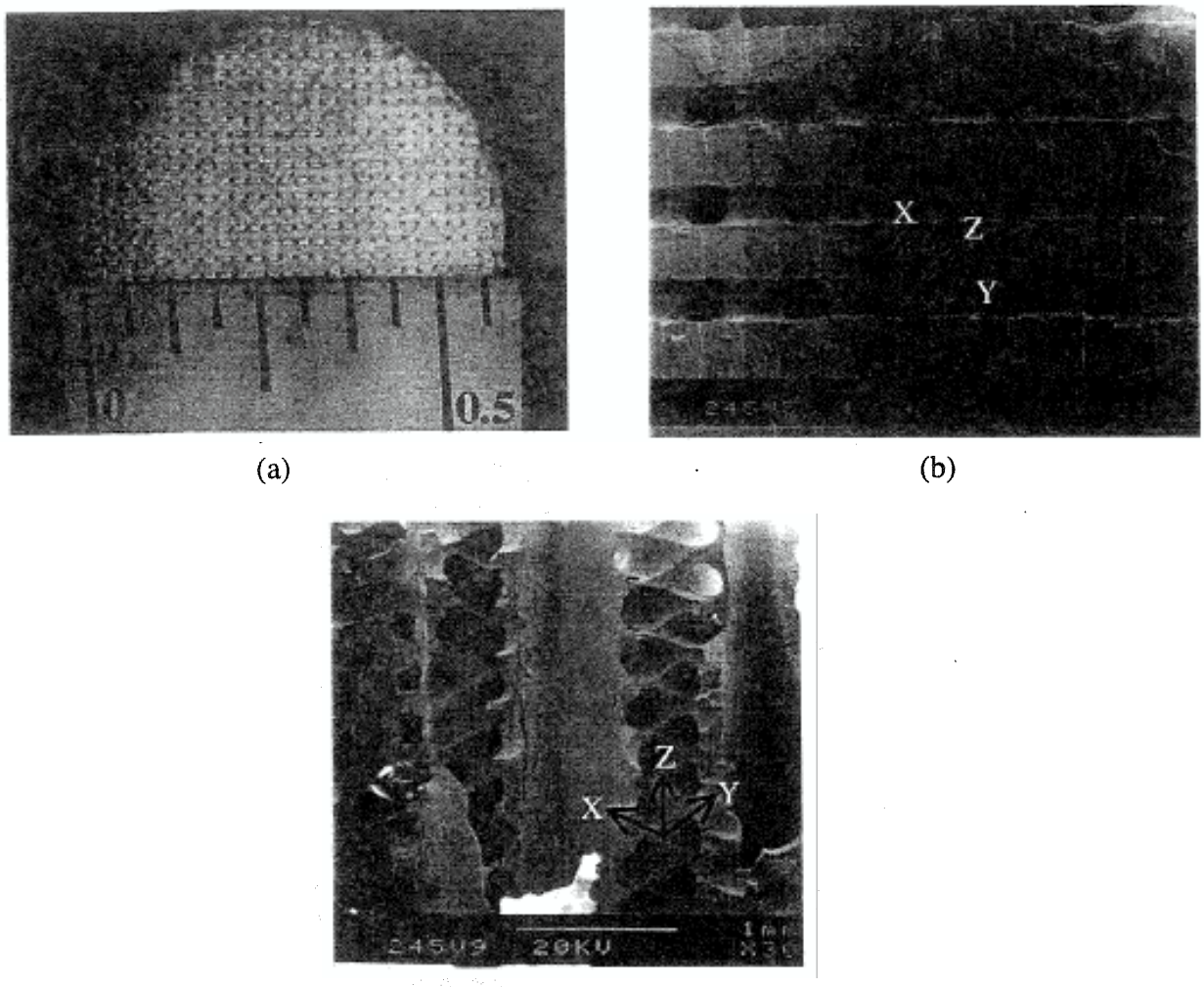

(a) (b)

(c)

Figure 6: Optical and SEM micrographs of the sintered alumina ceramic preforms. (a) Top view of a cylindrical sample (~0.6" diameter). (b) Top view of a ceramic preform with *uniform pore sizes* in X, Y and Z directions (~ 300μm diameter). (c) Side view of a ceramic preform with *non-uniform pore sizes* in X, Y and Z directions (~ 300μm diameter in X and Y and 750μm in Z).

Figure 6 shows the optical and scanning electron micrographs of samples with uniform and non-uniform pore sizes. 3D honeycomb structures with 33% to 50% total pore volumes were fabricated with pore sizes varying from 300 μm to 750 μm. Figure 6 (b) shows the SEM micrograph of the uniform pore size sample where ~300 μm diameter pores are interconnected in X, Y and Z directions. Figure 6 (c) shows another structure where pore sizes in Z direction is ~750 μm and ~300 μm in X and Y directions.

Initial compression tests were performed with some of these samples having 33% pore volume and uniform pore sizes using an MTS servo hydraulic machine. The compression test data is shown in Figure 7. These tests were performed with samples having a diameter vs. height ratio 1:1. The load vs. displacement curve showed a stepwise increase due to the failure of some of the pore walls during testing. The final fracture of these test samples occurred longitudinally with a multifaceted fracture surface. Final fracture stress varied between 2000 to 2500 MPa for samples with 33 volume% of porosity with pore sizes varying from 300 to 400 μm. Further compression tests and four point flexural tests of these samples are currently under investigation.

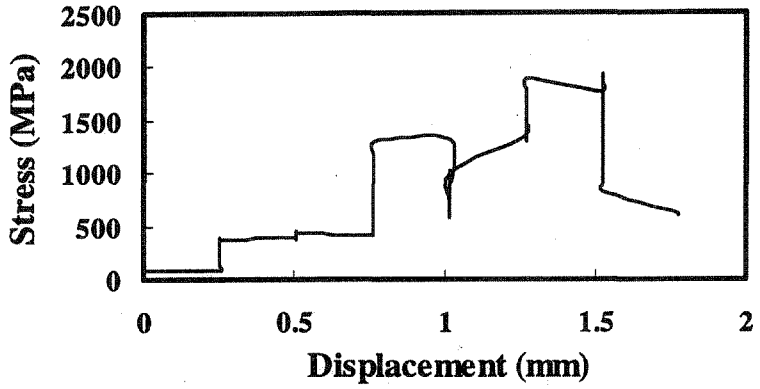

Figure 7: Displacement vs. stress plot for the 3-D honeycomb porous alumina ceramic preforms having 33% porosity.

Conclusions

3D honeycomb porous alumina ceramic preforms were fabricated using indirect SFF route. Polymeric molds were fabricated using FDM 1650 with ICW06 filaments and then infiltrated with ceramic slurry and then dried. Dry molds were subjected to a binder burn out and sintering cycle. Structures with uniform and non-uniform pore sizes were fabricated via this method. Initial compression tests of 33 volume % porous structures showed that ultimate failure stress varied in the range of 2000 to 2500 MPa. Detailed mechanical characterization of these samples is currently under investigation.

Acknowledgements

The authors would like to acknowledge John Merlino, Rubiela Diaz, Shinichi Sugiura and Sudharshan Rangaraj of the School of Mechanical and Materials Engineering at WSU for their help in SEM, and other materials processing work.

References

1. L. L. Hench, "Bioceramics: From Concept to Clinic," *J. Amer. Ceram. Soc.*, **74**[7], pp 1487-510 (1991).
2. L. L. Hench, "Bioceramics," *J. Amer. Ceram. Soc.*, **81**[7], pp 1705-28 (1998).
3. L. L. Hench and J. Wilson, "An Introduction to Bioceramics," World Scientific (1993).
4. A. Ravaglioli and A. Krajewski, "Bioceramics: Materials, Properties, Applications," Chapman and Hall, London, (1992).
5. K. deGroot, "Clinical Applications of Calcium Phosphate Biomaterials: A Review," *Ceramics International*, 19, pp 363-66 (1993).
6. H. Alexander, J. R. Parsons, J. L. Ricci, P. K. Bajpai and A. B. Weiss, "Calcium Based Ceramics and Composites in Bone Reconstruction," *CRC Critical Reviews in Biocompatibility*, 4 [1], pp 44 (1987).
7. L. L. Hench and E. C. Ethridge, "Biomaterials: An Interfacial Approach," Academic Press, New York, (1982).
8. G. Lee and J. W. Barlow, "Selective Laser Sintering of Calcium Phosphate Powders," Proceedings of the Solid Freeform Fabrications 1993, The University of Texas at Austin, TX, pp 191-97 (1993).
9. G. Lee, J. W. Barlow, W. C. Fox and T. B. Aufdermorte, "Biocompatibility of SLS formed Calcium Phosphate Implants," Proceedings of the Solid Freeform Fabrications 1996, The University of Texas at Austin, TX, pp 15-21 (1996).
10. US patent 5,518,680.
11. US patent 5,490,962.
12. T. M. Chu and J. W. Halloran, "Hydroxyapatite Scaffolds with Controlled Porosity," presented at the Bioceramics: Materials and Applications Symposium at 100th Annual American Ceramic Society Meeting, Cincinnati, OH, May 2-6, 1998.
13. R. Garg, R. K. Prud'homme and I. A. Aksay, "Orthopaedic Implants by Ceramic Stereolithography," presented at the Bioceramics: Materials and Applications Symposium at 100th Annual American Ceramic Society Meeting, Cincinnati, Ohio, May 2-6, 1998.
14. P. Teung, R. K. Panda, S. C. Danforth and A. Safari, "Fabrication of Porous Hydroxyapatite Ceramics by Solid Freeform Fabrication Technique," presented at the Bioceramics: Materials and Applications Symposium at 100th Annual American Ceramic Society Meeting, Cincinnati, OH, May 2-6, 1998.